UNIVERSITÀ DI PARMA
ARCHIVIO DELLA RICERCA

University of Parma Research Repository

Cyclosporine-loaded micelles for ocular delivery: Investigating the penetration mechanisms

This is the peer reviewd version of the followng article:

Original
Cyclosporine-loaded micelles for ocular delivery: Investigating the penetration mechanisms / Ghezzi, Martina; Ferraboschi, Ilaria; Delledonne, Andrea; Pescina, Silvia; Padula, Cristina; Santi, Patrizia; Sissa, Cristina; Terenziani, Francesca; Nicoli, Sara. - In: JOURNAL OF CONTROLLED RELEASE. - ISSN 1873-4995. - 349:(2022), pp. 744-755. [10.1016/j.jconrel.2022.07.019]

Availability:
This version is available at: 11381/2932464 since: 2024-12-12T15:37:08Z

Publisher:

Published
DOI:10.1016/j.jconrel.2022.07.019

Terms of use:

Anyone can freely access the full text of works made available as "Open Access". Works made available

Publisher copyright

note finali coverpage

(Article begins on next page)

11 January 2025

Cyclosporine-loaded micelles for ocular delivery: investigating the penetration mechanisms

Martina Ghezzi[1], Ilaria Ferraboschi[2], Andrea Delledonne[2], Silvia Pescina[1], Cristina Padula[1], Patrizia Santi[1], Cristina Sissa[2], Francesca Terenziani[2], Sara Nicoli[1]*

[1] ADDRes Lab, Department of Food and Drug, University of Parma, Parco Area delle Scienze 27/A, 43124 Parma, Italy

[2] Department of Chemistry, Life Science and Environmental Sustainability, University of Parma, Parco Area delle Scienze 17/A, 43124 Parma, Italy

*Corresponding Author:

Sara Nicoli PhD
ADDRes Lab (Advanced Drug Delivery Research Lab)
Department of Food and Drug
University of Parma
Parco Area delle Scienze, 27/A
43124 Parma, Italy
Telefono +39 0521 905065/71
Fax +39 0521 905006
E-mail: sara.nicoli@unipr.it

Submitted to: Journal of Controlled Release

Abstract:

Cyclosporine is an immunomodulatory drug commonly used for the treatment of mild-to-severe dry eye syndrome as well as intermediate and posterior segment diseases as uveitis. The ocular administration is however hampered by its relatively high molecular weight and poor permeability across biological barriers. The aim of this work was to identify a micellar formulation with the ability to solubilize a considerable amount of cyclosporine and promote its transport across ocular barriers. Non-ionic amphiphilic polymers used for micelles preparation were tocopherol polyethylene glycol 1000 succinate (TPGS) and Solutol® HS15. Furthermore, the addition of alpha-linolenic acid was assessed. A second aim was to evaluate micelles fate in the ocular tissues (cornea and sclera) to shed light on penetration mechanisms. This was possible by extracting and quantifying both drug and polymer in the tissues, by studying TPGS hydrolysis in a bio-relevant environment and by following micelles penetration with two-photon microscopy. Furthermore, TPGS role as permeation enhancer on the cornea, with possible irreversible modifications of tissue permeability, was analyzed. Results showed that TPGS micelles (approx. 13 nm in size), loaded with 5 mg/ml of cyclosporine, promoted drug retention in both the cornea and the sclera. Data demonstrated that micelles behavior strictly depends on the tissue: micelles disruption occurs in contact with the cornea, while intact micelles diffuse in the interfibrillar pores of the sclera and form a reservoir that can sustain over time drug delivery to the deeper tissues. Finally, cornea quickly restore the barrier

47 properties after TPGS removal from the tissue, demonstrating its potential good tolerability for
48 ocular application.
49
50 Keywords: cyclosporine, polymeric micelles, corneal delivery, transscleral delivery, TPGS hydrolysis,
51 two-photon microscopy
52
53 Highlights

54 • TPGS micelles improved cyclosporine solubility promoting its retention in eye tissues
55 • Micelles disassemble in contact with the cornea
56 • Micelles diffuse intact inside the scleral tissue
57 • TPGS is hydrolyzed by tissue esterases when in contact with cornea and sclera
58 • Two-photon microscopy is a useful tool to study micelles-tissues interaction

59
60

1. **Introduction**

Cyclosporine A (CYC), a neutral cyclic peptide isolated from different fungal species, is an immunomodulatory drug which works inhibiting T cells activation by blocking the transcription of cytokine genes including those encoding for IL-2 and IL-4 [1]. Its main ocular application is the treatment of mild-to-severe dry eye syndrome (DES) and, with this indication, it is present as anionic O/W emulsion on the US market (0.05%, Restasis®) and as a cationic O/W nanoemulsion (0.1%, Ikervis®) on EU market. Moreover, an ophthalmic solution (0.09%, Cequa®) has been recently approved by the Food and Drug Administration. Together with the treatment of DES and other corneal affections [2, 3], cyclosporine has demonstrated its activity for the treatment of blepharitis [4, 5] as well as intermediate and posterior segment diseases including uveitis [6, 7] and Behçet disease [8].

The formulation of this drug and its delivery to ocular tissues are however hampered by its relatively high molecular weight (1202.6 g/mol), poor water solubility [9] and marked lipophilicity (log P= 3 [10]). Therefore, cyclosporine A is mainly administered via oily and surfactant-containing formulations [11], presenting low tolerability and side effects, such as ocular burning, vision interference, eye irritation and conjunctival hyperaemia [9, 12]. Moreover, cyclosporine higher affinity for the oily phase rather than the aqueous environment usually results in a poor bioavailability [12]. A possible alternative to solve these issues is represented by the use of micelles, i.e. colloidal systems formed by self-assembling of amphiphilic molecules ~~polymers~~ in solution at a concentration above the Critical Micellar Concentration (CMC). Surfactant micelles, made by low molecular weight compounds, show high CMC and thus low physical stability. On the contrary, polymeric micelles, i.e. micelles formed by amphiphilic polymers, are characterized by lower CMC and better stability against dilution, and are generally preferred as drug delivery systems. Micelles are composed of an inner lipophilic core, involved in drug loading and release, and an external hydrophilic shell, responsible for micelles interaction with body targets. These nanosystems, in addition to a relatively easy preparation, sterilization method and high scale-up feasibility, showed good solubilization properties and efficient cellular internalization [13-15]. In case of ocular delivery, micelles have demonstrated the ability to enhance drug transport to the anterior eye segment [16-18] thanks to an improved solubility of drugs, higher penetration capacity (due to their nanometric size) and prolonged drug release [19-21]. Furthermore, ex-vivo data highlighted their capability to promote drug permeation across ocular tissues such as the sclera and the choroid, in the perspective of a posterior segment targeting [16, 21, 22]. It is also worth mentioning that an extremely recent review identifies the word “micelles” as one of latest high-frequency keywords, including this vehicle among the emerging frontiers in ocular drug delivery [23]. Unfortunately, the intense academic research has not necessarily been followed by actual industrial development. The reasons are different, related to stability problems and difficulty of characterization [13, 24], but also to the scarce information available regarding the fate of the polymer following ocular administration. This aspect should be investigated since it provides numerous information: first of all, the quantification of the polymer in the various tissues allows us to elucidate the transport mechanisms, a non-trivial action in the case of micelles that, being association colloids, can undergo considerable and rapid changes following interaction with biological fluids and tissues. Alongside this aim, to follow the "destiny" of the polymer is extremely important under a toxicological point of view: this is

103 particularly relevant when the target is represented by the posterior segment of the eye, because
104 in this case a contact between the polymer and the retina can be envisaged.
105
106 Thus, the idea behind this work was to identify a micellar formulation with the ability to solubilize a
107 relevant amount of cyclosporine and promote its transport across ocular barriers. Non-ionic
108 amphiphilic polymers used for micelles preparation were tocopherol polyethylene glycol 1000
109 succinate (TPGS) and Solutol® HS15. Furthermore, the addition of alpha-linolenic acid was assessed,
110 in the light of the interesting results reported on fatty acids for micelles preparation [25, 26] and
111 increased drug loading [27, 28]. A second aim was to evaluate micelles fate in the ocular tissues
112 (cornea and sclera) to shed light on the penetration mechanisms. This was possible by quantifying
113 both drug and polymer in the tissues, by studying TPGS hydrolysis in a bio-relevant environment
114 and by following micelles penetration with two-photon microscopy.

115 **2. Materials and methods**
116
117 **2.1. Materials**
118
119 Cyclosporine A (MW 1202.6 g/mol; logP 3; water solubility 27.67 µg/ml [29]) was purchased from
120 Alfa Aesar (Kandel, Germany) while tocopheryl polyethylene glycol 1000 succinate (TPGS) was
121 received from PMC ISOCHEM (Vert-Le-Petit, France). Alpha-linolenic acid (LA; MW 278.43 g/mol;
122 logP 6.46; pK_a 4.77), fluorescein sodium (MW 376.28 g/mol) and Nile red (NR; 9-(diethylamino)-5H-
123 benzo[a]phenoxazin-5-one; MW 318.4 g/mol) were purchased from Sigma-Aldrich (Saint Louis, MO,
124 USA). Solutol® HS15 was received from BASF (Ludwigshafen, Germany) whereas citric acid and
125 propylene glycol were purchased from A.C.E.F. S.p.a (Fiorenzuola d'Arda, Italy). For HPLC analysis
126 high purity water (Purelab® Pulse, Elga Veolia,UK) and HPLC grade acetonitrile were used. Acetate
127 buffer was prepared by mixing 0.1 M acetic acid and 0.1 M sodium acetate solutions in 82:18 (v/v)
128 ratio; pH was adjusted to 4.8 using 0.1 M NaOH. Simulated tear fluid (STF) was obtained by
129 solubilizing in water $CaCl_2$ 0.06 g/l, $NaHCO_3$ 2.18 g/l and NaCl 6.7 g/l; pH was adjusted to 7.4 using
130 1M HCl. Phosphate Buffer Saline (PBS) was prepared by dissolving in high purity water KH_2PO_4 0.19
131 g/l, Na_2HPO_4 2.37 g/l and NaCl 8.8 g/l; pH was adjusted to 7.4 using H_3PO_4 85%. HEPES buffer was
132 prepared by solubilizing in high purity water HEPES 5.96 g/l and NaCl 9 g/l; pH was adjusted to 7.4
133 using NaOH 5M.
134
135 **2.2. Cyclosporine and linolenic acid quantification method**
136
137 Cyclosporine and linolenic acid quantification was performed using an HPLC-UV system (Infinity
138 1260, Agilent Technologies, Santa Clara, CA, USA), with a reverse-phase column (Aeris™ WIDEPORE
139 XB-C_8 column, 150 x 4,60 mm, 3,6 µm, Phenomenex, Torrance, CA, USA) thermostated at 65°C. The
140 mobile phase was composed of CH_3CN:water with TFA 0.1% in ratio 55:45 (v/v). The flow was
141 maintained at 1.6 ml/min and the injection volume was equal to 100 µl. The retention time of
142 cyclosporine and linolenic acid, both quantified by UV absorbance at 230 nm, was respectively of
143 4.9 and 3.1 minutes. For cyclosporine, linearity was found in the interval 1-50 µg/ml, whereas for

linolenic acid in the range 5-100 µg/ml. Details on calibration curves, RSD%, RE% and LOQ values, as well as discussion on the method and the impact of the injection solvent are reported in the supplementary materials (see par. 1.1).

2.3. TPGS quantification method

TPGS quantification, performed with a previously validated method [30], was done using an HPLC-UV system (Infinity 1260, Agilent Technologies, Santa Clara, CA, USA), with a reverse-phase C18 column (Waters, Symmetry300 C18, 5 µm, 4.6 × 250 mm) and a C18 guard column (SecurityGuard Widepore C18, Phenomenex, Torrance, CA, USA), thermostated at 40 °C. The mobile phase, composed of acetate buffer pH 4.8:CH_3OH in 3:97 (v:v) ratio, was pumped at 2 ml/min. The retention time of TPGS, quantified by UV absorbance at 215 nm, was 4 minutes while the injection volume was 100 µl. Calibration curves were built in the concentration interval 1-25 µg/ml. Samples were injected without previous dilution. Further information on the preparation of the standards for the calibration curve are reported in the supplementary materials (see par. 1.2).

2.4. Preparation of blank polymeric micelles

Polymeric micelles were prepared by direct dissolution of TPGS and/or Solutol® HS15 in high purity water to obtain formulations S (Solutol®), ST (Solutol® and TPGS) and T (TPGS) (see Figure 1 for details on the structure and table 1 for details on the composition of micellar formulations).

Figure 1: Drug and excipients used for micelles preparation with their main chemical features and molecular structure.

Compound	Molecular weight (g/mol)	Log P	HLB	pK_a	H-bond capacity (donor-acceptor)	Molecular structure
Cyclosporine	1202.6	2.92	-	13.3	5-12	
TPGS	1513	-	13.2	-	1-6	n=23
Solutol® HS15	963.2	-	14-16	-	3-19	n=12
Linolenic acid	278.4	6.46	-	4.77	1-2	

8 ml of S, ST and T micelles were then added with 100 µl of linolenic acid (L) this becoming SL, STL, TL, respectively, and vortexed (3 times x 20 sec each) in order to ensure complete saturation of the aqueous phase. Afterwards, to separate linoleic acid and obtain a clear solution, the oily phase was removed by 2-folds filtration (regenerated cellulose, Sartorius Minisart RC 0.2 µm). The amount of

172 linolenic acid loaded in the micelles was then evaluated by HPLC after proper dilution with the
173 mobile phase.
174
175 Table 1: Blank micellar formulations with relative composition and codification.

CODE	TPGS (mM)	SOLUTOL® HS15 (mM)	LINOLENIC ACID
T	20	-	-
S	-	20	-
ST	10	10	-
TL	20	-	at saturation
SL	-	20	at saturation
STL	10	10	at saturation

176
177 **2.5. Cyclosporin-loaded polymeric micelles**
178
179 In order to determine cyclosporine solubility, the blank micellar formulations (see table 1 for the
180 compositions) were added with an excess of the drug, sonicated for 3 minutes and left under
181 magnetic stirring at room temperature for at least 72 h. Then, the suspension was centrifuged at
182 10,000 rpm for 15 minutes and, when needed, for other 20 minutes at 15,000 rpm to get complete
183 precipitation of the undissolved drug and obtain a limpid formulation. The supernatant was sampled
184 and analyzed by HPLC-UV for determining the solubility of both cyclosporine and linolenic acid after
185 proper dilution with the mobile phase. Cyclosporine solubility is reported as mean ± SD; n ≥ 9 for T
186 micelles, n ≥ 3 for the other formulations.
187 Size and polydispersity index (PDI) of blank and CYC-loaded micelles were measured by Dynamic
188 Light Scattering (DLS) using a Zetasizer Nano-ZSP (Malvern Instruments, Malvern, UK).
189 Measurements were performed at 25 °C after 10-folds dilution in high purity water.
190
191 **2.6. Tissue preparation**
192
193 Fresh porcine eyes were isolated from Landrance and Large White (age 10–11 months, weight 145–
194 190 kg), female and male animals supplied from a local slaughterhouse (Macello Annoni S.p.A.,
195 Parma, Italy). The eyes were kept in PBS at 4 °C until the dissection, which occurred within 2 h from
196 the enucleation. The muscular and connective tissues around the eye bulb were completely
197 removed. For corneal permeation experiments, only bulbs with macroscopically intact corneas were
198 used, whereas eyes showing opaque corneas were discarded. The cornea, isolated as a corneo-
199 scleral button-shaped piece, was obtained cutting with a scalp beyond the limbus. For scleral
200 permeation, the isolated sclera was obtained by circumferentially cutting and removal of the
201 anterior segment of the eye behind the limbus. The collected eyecup was then cut and everted. The
202 neural retina and the choroid-Bruch's layer were discarded while the sclera was used for the
203 permeation experiment.
204
205 **2.7. Study of the effect of TPGS on cornea permeability: transcorneal permeation of**
206 **fluorescein**
207

208 In order to evaluate if TPGS induces an increase of corneal permeability, the permeation of sodium
209 fluorescein was evaluated after application of TPGS micelles to the tissue for 10 minutes. The tissue
210 was mounted on a glass Franz-type vertical diffusion cell (DISA, Milano, Italy) with a permeation
211 area of 0.2 cm^2. The receptor was filled with HEPES buffer pH 7.4 (about 4 ml, exactly measured)
212 magnetically stirred at 37°C to guarantee sink conditions. First, the donor was pre-treated with 200
213 µl of TPGS 20 mM micelles for 10 min. Afterwards, the formulation was removed and the tissue was
214 washed 3 times with 200 µl of HEPES buffer and carefully dried with a cotton swab. A solution of
215 fluorescein sodium (1.18 mg/ml) was then applied at infinite dose (200 µl/cm^2) for 4 h. 300 µl of
216 receptor solution were sampled at different timepoints (0, 1, 1.5, 2, 3 and 4 hours from the
217 deposition of the formulation) and the receptor was filled with fresh HEPES buffer. Negative and
218 positive controls were also evaluated. The negative control was represented by a pre-treatment of
219 10 minutes with HEPES buffer (pH 7.4). The positive control was represented by a 0.1% p/v
220 benzalkonium chloride solution applied for 5 or 10 minutes.
221 The samples fluorescence (λ_{exc}=490 nm, λ_{em}=535 nm) was measured via microplate reader (SPARK10
222 M, TECAN, Mannendorf, CH). More information on the preparation of the calibration curve, RSD%,
223 RE% and LOQ values are reported in the supplementary materials (par. 1.3). All experiments were
224 carried out using different ocular bulbs from different animals. The amount of fluorescein sodium
225 permeated (µg/cm^2) was reported as a function of time (min). The transcorneal flux across the
226 cornea (J, µg/cm^2h) was determined as the slope of the regression line at the steady state, while the
227 apparent permeability coefficient (P, cm/s) was calculated at the steady state as: $P=J/C_d$, where C_d
228 (µg/ml) is the concentration of the donor solution. Data are reported as mean ± SD; number of
229 replicates was n ≥ 3, unless differently indicated.
230
231 **2.8. Retention and permeation experiments across cornea and sclera**
232
233 The tissue was mounted on a glass Franz-type vertical diffusion cell (DISA, Milano, Italy) with a
234 permeation area of 0.2 cm^2 (cornea) or 0.6 cm^2 (sclera). The set-up used for corneal permeation
235 experiments was previously validated to guarantee that tissue barrier properties were preserved
236 throughout the experiment duration [31]. The receptor was filled with PBS pH 7.4 (4 ml, exactly
237 measured) that was magnetically stirred to guarantee sink conditions. The formulations were
238 applied at infinite dose (200 µl/cm^2, occluded). At the end of the experiment, the receptor solution
239 was sampled, the formulation was removed from the donor and the tissue was rinsed 3 times with
240 PBS. Therefore, cyclosporine and TPGS were extracted by treating tissues with 1 ml solution of
241 CH_3CN:CH_3COOH 1% in 87:13 ratio. Samples were left under these conditions overnight at room
242 temperature, then sonicated for 12 minutes and centrifuged at 12,000 rpm for 15 min before HPLC
243 analysis. This extraction method, previously validated for cyclosporine [30], was also challenged for
244 its ability to extract TPGS. The percentage of recovery found for TPGS was 91.9 ± 3.15 %. In case of
245 cornea, experiment duration was 5 h and CYC-loaded formulations tested were T, TL and ST (see the
246 composition in Table 1 and CYC solubility in Figure 2). In case of sclera, only T was evaluated. The
247 experiments were performed for 6 and 48 h. Additionally, to evaluate the reservoir effect of the
248 tissue, T was applied to the sclera for 6 h; then, the formulation was carefully removed, the sclera
249 surface was dried with a cotton bud and permeation experiment was continued up to 48 h. After

250 this time, cyclosporine was extracted from the sclera and quantified in the receptor phase, as
251 previously described. Data are reported as mean ± SD; n ≥ 3 for all formulations.
252
253 **2.9. Hydrolysis of TPGS in contact with ocular tissues**
254
255 The in vitro enzymatic hydrolysis of TPGS was evaluated using cornea and sclera excised from fresh
256 porcine eyes. In particular, the isolated tissues were punch-biopsied with a 0.9 mm punch and cut
257 in four pieces of the same size.
258 A solution of TPGS with concentration 100 µg/ml was prepared by dissolving the polymer in a
259 mixture of PBS pH 7.4:water in ratio 1:10. Then, 300 µl of TPGS 100 µg/ml were incubated with two
260 pieces of the tissue (average weight 50 mg for cornea and 60 mg for sclera) for 24 h (for the cornea)
261 and 48 h (for the sclera) at 37°C. At predetermined time intervals, samples were centrifuged at
262 12,500 rpm for 5 minutes and 40 µl of the TPGS solution were withdrawn and diluted 1:10 with
263 CH_3CN:CH_3COOH 1% (87:13), causing esterase inactivation. The concentration of TPGS in these
264 samples was measured by HPLC. Control samples obtained in the same conditions but without tissue
265 were analyzed as well.
266
267 **2.10. Two-photon microscopy**
268
269 For the two-photon microscopy analysis, Nile red-loaded TPGS 20 mM micelles were prepared.
270 Briefly, 10 µl of a 10 mg/ml NR solution in DMSO were added to 1.5 ml of blank TPGS 20 mM
271 micelles. The sample was then centrifuged at 13,000 rpm for 5 min to precipitate the exceeding NR
272 and to collect the supernatant. Afterwards, the corneal or the scleral tissue was mounted on a Franz-
273 type vertical diffuse cell (0.6 cm^2). The donor was filled with 120 µl of NR-loaded TPGS micelles,
274 while the receptor was filled with PBS pH 7.4 under magnetic stirring. The experiment duration was
275 2 h. The same experiment was performed also using a reference NR saturated aqueous solution
276 prepared by adding 10 µl of a 10 mg/ml NR solution in DMSO to 1.5 ml of high purity water and
277 centrifuging following the conditions previously reported to collect the supernatant.
278 Porcine samples were analyzed with a Two-Photon Microscope Nikon A1R MP+ Upright equipped
279 with a femtosecond pulsed laser Coherent Chameleon Discovery (~ 100 fs pulse duration with 80
280 MHz repetition rate, tunable excitation range 660-1320 nm). A 25× water dipping objective with
281 numerical aperture 1.1 and 2-mm working distance was employed for focusing the excitation beam
282 and for collecting the two-photon excited fluorescence (TPEF) and the second harmonic generation
283 (SHG) signals. TPEF/SHG signal was directed by a dichroic mirror to a series of three non-descanned
284 detectors (high sensitivity GaAsP photomultiplier tubes) allowing fast image acquisition. The three
285 detectors are preceded by optical filters allowing the simultaneous acquisition of three separated
286 channels: blue channel (415–485 nm), green channel (506–593 nm) and red channel (604–679 nm).
287 Imaging overlay of the three channels and processing was performed by the operation software of
288 the microscope. Additionally, a fourth GaAsP photomultiplier detector, connected to the
289 microscope through an optical fiber and preceded by a dispersive element, was used to record the
290 spectral profile of the TPEF/SHG signal (wavelength range 430 to 650 nm with a bandpass of 10 nm).

For microscope observations, performed right after dismounting the tissue from the Franz-type cell, the samples were placed in a dedicated plexiglass holder and saline solution was used to dip the objective and to avoid dehydration. Two different excitation wavelengths were used, 860 or 1080 nm. Images were acquired with a typical field of view of 500 μm × 500 μm, except where explicitly reported.

Besides two-photon microscopy analysis, the emission spectrum of NR-loaded TPGS micelles and a NR solution in water were registered with an Edinburgh FLS-1000 fluorimeter. The solutions were prepared by adding 20 μL of a 400 μM DMSO NR stock solution in 3 mL of 0.5 mM TPGS micelles or high purity water (final NR concentration 2.7 μM, total percentage of DMSO < 1%) which were then filtered after the preparation (hydrophilic PTFE, AISIMÔ 0.22 μm).

2.11. Statistical analysis

All data presented in text, figures and tables are reported as mean value ± SD. The significance of the differences between the results was assessed using Student's t-test. Differences were considered statistically significant when $p < 0.05$.

3. Results and discussion

Polymeric micelles have demonstrated to be powerful tools to overcome the drawbacks of traditional ocular dosage forms, with particular potentialities for an improved drug administration to the anterior segment of the eye. Indeed, micelles can be used to formulate hydrophobic compounds as aqueous solutions which, applied as eye drops, can easily mix with the lacrimal fluid without causing any vision interference [14, 32].

3.1. Cyclosporine solubility studies

The first part of the work was dedicated to the identification of micellar formulas capable of increasing cyclosporine aqueous solubility, that is very low; in simulated tear fluid we found a solubility lower than 5 μg/ml.

The polymers used were TPGS and Solutol® HS15, alone or combined in a 1:1 molar ratio. TPGS, was selected for the possible release of antioxidant vitamin E via enzymatic hydrolysis [30]. Moreover, this polymer previously demonstrated its permeation enhancing properties for several drugs through the corneal tissue [33-35] probably related also to P-glycoprotein inhibition [36]. Solutol® HS15 was selected considering its capacity to improve hydrophobic drugs solubility [37, 38] and its promising outcomes regarding the enhancement of corneal permeability and retention [39]. Linolenic acid was also added to the micellar formulations (see table 1 for detailed composition and codification) since data previously collected in our laboratory demonstrated the capability of fatty acids to increase the encapsulation of an hydrophobic compound [27]. Additionally, linolenic acid is a precursor of prostaglandin E1, a potent anti-inflammatory agent capable of reducing the ocular inflammation [40], promoting tear production and decreasing DES symptoms [41]. Some studies demonstrated that dietary supplementation with linolenic acid led to a reduction of ocular surface

inflammation in patients with DES [42, 43] and there is also some evidence of omega-3 fatty acids effectiveness when applied topically [44, 45].

TPGS and Solutol® demonstrated a similar capability to dissolve linolenic acid (4 mg/ml). However, their 1:1 mixture reduced linolenic acid solubility by half. Cyclosporine was then added to the micelles; TPGS alone gave the highest cyclosporine solubility (5.26 ± 0.39 mg/ml) and Solutol® the lowest (0.57 ± 0.1 mg/ml). In the presence of linolenic acid, the solubility of cyclosporine decreased (Table 2) regardless the polymers composition. Also the concentration of linolenic acid after cyclosporine loading (Table 2) showed to be markedly reduced by cyclosporine presence; this suggests a competition between the two molecules for the interaction with the micellar core, whose size is relatively small [27]. This result differs from the previously published data on imiquimod, where fatty acids co-encapsulation was used to increase the solubility of this hydrophobic drug into TPGS micelles [27].

Table 2. Solubility of cyclosporine (CYC) and linolenic acid (LA) alone and combined in the micellar formulations. Formulations further evaluated are indicated in bold.

	FORMULATION	CYC SOLUBILITY (mg/ml)	LA SOLUBILITY (mg/ml)
cyclosporine only	T	5.26 ± 0.39	-
	S	0.57 ± 0.1	-
	ST	3.27 ± 0.28	-
linolenic acid only	TL	-	3.82 ± 0.11
	SL	-	4.26 ± 0.32
	STL	-	2.37 ± 0.31
cyclosporine and linolenic acid	TL	3.04 ± 0.52	0.60 ± 0.03
	SL	n.d.	n.d.
	STL	0.53 ± 0.09	1.240.25

Given the results obtained, the formulations T, TL and ST loaded with cyclosporine were selected for further studies, since they guarantee a drug solubility equal or higher than 3 mg/ml and, in the case of TL, also the presence of linolenic acid that can support drug action. Additionally, these formulations were selected also for their stability, evaluated after approx. 2 months as reported in Figure S2.

The size of the drug-loaded micelles, reported in Table 3, is between 13 and 16 nm. Details on DLS analysis including data on discarded formulations and blank micelles are presented in supplementary material (Table S2). The size of TPGS as well as Solutol® micelles demonstrated to be in good agreement with values reported in the literature [46, 47] and minor changes in micelle size were reported after addition of linolenic acid or after cyclosporine loading, despite the increase in the polydispersity index.

363 **3.2. Cyclosporine and TPGS accumulation and retention in ocular tissues**

364 The role of the micellar formulation on drug delivery to the ocular structures has not been fully
365 clarified. An increased solubility, the permeation enhancing properties of the polymer and the
366 uptake of intact micelles seem to concur to the increased drug penetration [48], however, the
367 contribution of each mechanism is difficult to deduce. In fact, given the nature of these nanocarriers,
368 formed by an association of amphiphilic unimers, the study of the interaction with the biological
369 environment is particularly hard. In this paper, to elucidate the micelles behaviour upon contact
370 with the biological barriers, we quantified both drug and polymer (TPGS) inside the ocular
371 structures.

372

373 **3.2.1. Cyclosporine and TPGS retention into the cornea**

374 Formulations T, TL and ST loaded with CYC at saturation were then applied to the corneal tissue to
375 evaluate their capability to promote drug uptake into the epithelial cells. At the end of the
376 experiment, the drug was extracted from the tissue with a validated method [30]. This method was
377 also challenged for its ability to extract TPGS that can likewise accumulate in the cornea. The results
378 obtained in term of cyclosporine and TPGS accumulation from these formulations are presented in
379 Table 3, while the amount of polymer and drug permeated is not reported as no transcorneal
380 permeation occurred.

381

382 Table 3. Composition, size and CYC solubility of the CYC-loaded micellar formulations evaluated on the corneal tissues.
383 Data on drug and TPGS accumulation in the cornea are also reported.

Micelles characteristics				Cyclosporin and TPGS delivery to the cornea	
	Composition	Size (nm) *(PDI)*	Cyclosporine conc. (mg/ml)	Cyclosporine in corneal tissue (μg/cm^2)	TPGS in corneal tissue (μg/cm^2)
T	TPGS 20 mM	12.96 ± 4.03[46] *(0.091)*	5.26 ± 0.39	19.81 ± 4.49	55.92 ± 26.25
TL	TPGS 20 mM saturated with linolenic acid	14.47 ± 4.91 *(0.196)*	3.04 ± 0.52 (linolenic acid: 0.60 ± 0.03)	2.82 ± 1.43	41.05 ± 22.92
ST	TPGS 10 mM and Solutol® 10 mM	15.65 ± 5.90 *(0.213)*	3.27 ± 0.28	2.35 ± 0.66	2.82 ± 0.08

384

385 Formulation T outperformed the others, with an amount of drug accumulated about 7-fold higher.
386 Both the addition of linolenic acid (TL) or Solutol® (ST) decreased micelles delivery efficiency. The
387 reason can only partially be attributed to the different drug concentration (5 vs 3 mg/ml), since all
388 the formulations are at the saturation level and the thermodynamic activity is comparable in all
389 cases. The TPGS concentration in the formulation (20 vs 10 mM) can contribute to partially explain
390 the result, since TPGS has widely demonstrated its permeation enhancing capacity resulting from
391 efflux pumps inhibition and also from the ability to interpose between the phospholipidic bilayers
392 of cellular membranes modifying their fluidity [33, 49]. To shed light on micelles permeation
393 mechanisms, we also quantified the amount of TPGS in the cornea. The accumulation of TPGS in the

absence of Solutol® (T and TL) gave high and comparable results, even if ~~showing~~ it presents high variability. The presence of Solutol® markedly decreased TPGS uptake, partially due to the lower concentration (10 vs 20 mM) and potentially also to a lower mobility of TPGS in the presence of mixed micelles, as previously demonstrated in the presence of poloxamers [46].
Since the TPGS:cyclosporine weight ratio in the T micelles is approximately 6:1, the data of corneal retention suggest that the micelles do not penetrate intact in the tissue; the drug is probably released as the micelles come in contact with the epithelial cells. There are however other phenomena to be considered, since TPGS could be metabolised in the tissue (see par 3.3).

Concerning the relevance of the corneal concentration obtained, we can compare our data with the ones previously obtained with the commercial formulation Ikervis®, a cationic nanoemulsion accumulating a cyclosporine amount of 0.60 ± 0.14 $\mu g/cm^2$ [30]. Considering the lower concentration of cyclosporin in Ikervis® (1 mg/ml), its performance is comparable with TL and ST, while formulation T markedly enhanced drug uptake. This can be relevant, considering the growing use of cyclosporine for diseases other than DES [50], that could require higher tissue concentration.

3.2.2. Cyclosporine and TPGS diffusion across the sclera from micellar formulations

In the last years, the topical route has been proposed for the administration of therapeutics also to the posterior segment of the eye. This topic is still under investigation: some researchers have actually highlighted the presence of the drug in the retina, but the clinical significance of the concentrations found is still subject of debate. The first barrier encountered by the formulation after topical application is the conjunctiva, which plays a crucial role as it mediates the delivery to the posterior segment (conjunctival–scleral route), but also the nonproductive and undesirable systemic absorption. Cyclosporine permeation across the conjunctiva from TPGS micelles was studied in a previous work [46]. The results highlighted the capability of both drug and TPGS to cross the conjunctival epithelium in significant amount. However, it is worth mentioning that the fast nasolacrimal clearance from the conjunctival sac as well as the systemic uptake mediated by blood and lymphatic vessels reduce the residence time on the eye surface to few minutes, making the achievemt of therapeutic concentrations in the posterior segment unlikely. A possible alternative is a subconjunctival administration, where the formulation is applied on the surface of the sclera. Although this procedure cannot be defined non-invasive, it avoids the most serious side effects connected with the intravitreal injection and, in the presence of a controlled-release formulation, can reduce the administration frequency. Also in this case, several static, dynamic and metabolic barriers strongly reduce drug absorption [51], therefore, in order to achieve therapeutic concentrations at the posterior ~~chamber~~ segment, ~~topical~~ formulations with high concentration of the drug are required.
T micelles, having the higher cyclosporine concentration among the formulations prepared, were selected for further studies regarding scleral accumulation and permeation. The donor was applied for 6 h or 48 h and, at the end of the experiment, both the drug and TPGS were quantified in the receptor phase and inside the scleral tissue. In order to investigate the “reservoir effect” of the scleral tissue (i.e. the capability to accumulate the drug and then slowly release it to the deeper

tissues), the donor was also applied for 6 hours, then removed and the experiment was continued up to 48 h. Results of drug and TPGS accumulation and permeation are listed in Figure 2.
The amount of cyclosporine recovered in the sclera after the 6 h treatment was much higher than in the cornea (87.75 ± 21.69 μg/cm^2 vs. 19.81 ± 4.49 μg/cm^2), in agreement with the different tissue structure, with the sclera being a permeable connective tissue made of collagen fibres. However, also in this case, no drug was detected in the receptor phase after 6 h from donor deposition.
Cyclosporine accumulation increases over time, from 87.75 ± 21.69 μg/cm^2 after 6 h of contact to 304.86 ± 13.39 μg/cm^2 after 48 h of contact. In this last case, it was also detected in the receptor compartment, in a very significant amount. When the donor was applied for 6 h and then removed, the total amount recovered after 48 h was very similar with respect to the 6 h experiment, but with a different distribution: while after 6 h the 100% of the drug was localized in the sclera, after 48 h the 15% permeated the tissue, demonstrating the capability of the sclera to slowly release the drug and/or the micelles into the deeper tissues.
The fate of TPGS was also followed. The amount recovered in the sclera after 6 h was approximately 500 μg/cm^2. Interestingly, when the donor was applied for 6 h and the quantification was made after 48 h, the amount of TPGS decreased to approximately 300 μg/cm^2. This reduction can be attributed to an esterase-mediated hydrolyzation of TPGS with consequent release of vitamin E [30] and will be further studied.

A

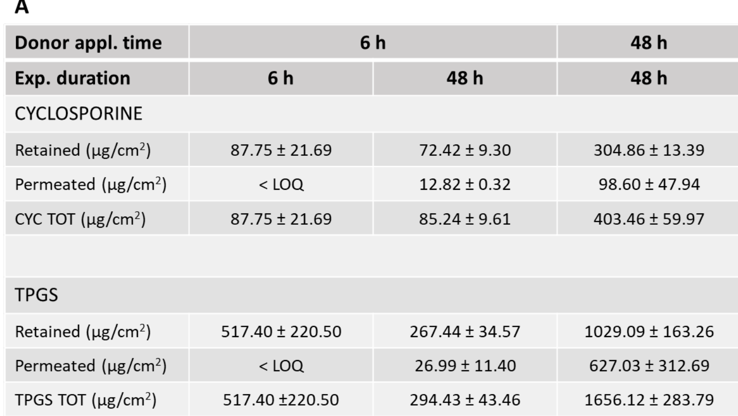

Donor appl. time	6 h		48 h
Exp. duration	6 h	48 h	48 h
CYCLOSPORINE			
Retained (μg/cm^2)	87.75 ± 21.69	72.42 ± 9.30	304.86 ± 13.39
Permeated (μg/cm^2)	< LOQ	12.82 ± 0.32	98.60 ± 47.94
CYC TOT (μg/cm^2)	87.75 ± 21.69	85.24 ± 9.61	403.46 ± 59.97
TPGS			
Retained (μg/cm^2)	517.40 ± 220.50	267.44 ± 34.57	1029.09 ± 163.26
Permeated (μg/cm^2)	< LOQ	26.99 ± 11.40	627.03 ± 312.69
TPGS TOT (μg/cm^2)	517.40 ±220.50	294.43 ± 43.46	1656.12 ± 283.79

B

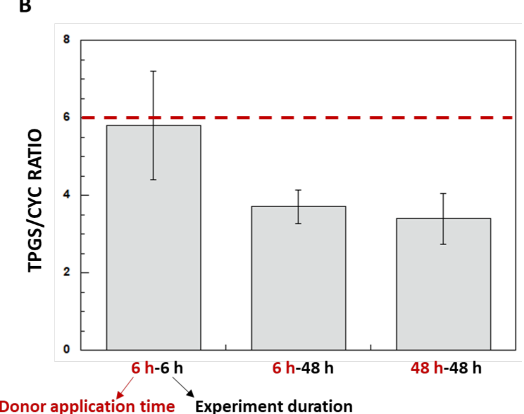

Figure 2. Panel A shows the amount of cyclosporine and TPGS accumulated in the sclera and permeated across the sclera (average ± SD) after formulation application in infinite dose conditions for 6 h and 48 h. The reservoir effect was also evaluated by removing the donor after 6 h and continuing the experiment for up to 48 h. Panel B represents TPGS/CYC ratio related to the amount accumulated inside the sclera following different donor application times and experiment durations. The red line shows the TPGS/cyclosporine ratio (TPGS/CYC) in the T formulation.

The quantification of TPGS gives the possibility of investigating the mechanisms of micelles penetration. The ratio between TPGS (30 mg/ml) and cyclosporine (5 mg/ml) in T micelles is approximately 6 (dotted line in Figure 2B). We have then considered drug and TPGS recovered (accumulated + permeated) at the end of each experiment and calculated this ratio. The result, presented in Figure 2, panel B, shows that the TPGS/cyclosporine ratio of the formulation is maintained in case of 6 h experiment duration suggesting that both the polymer and the drug are permeated together in form of intact micelles. This is reasonable, if considering the small size of this nanocarriers and the relatively high porosity of the sclera. The reduced polymer/drug ratio

470 registered for the other experimental conditions can be attributed to TPGS hydrolysis taking place
471 in the scleral tissue and particularly evident at long contact times (see par 3.3).
472
473
474 **3.3. TPGS metabolism in contact with ocular tissues**
475
476 Previous studies [30, 52] indicate that TPGS, which is stable in solution between pH 4.5 and 7.5, can
477 be hydrolyzed to vitamin E and vitamin E succinate in the presence of esterases, enzymes
478 ubiquitously present in tissues and also in the porcine [54] and human [53, 55] cornea and sclera.
479 However, at the best of our knowledge, the hydrolysis of TPGS in contact with ocular tissues has
480 never been studied before. This point is relevant since TPGS degradation could cause a reduction or
481 even loss of the micelles self-assembling properties promoting drug release.
482
483

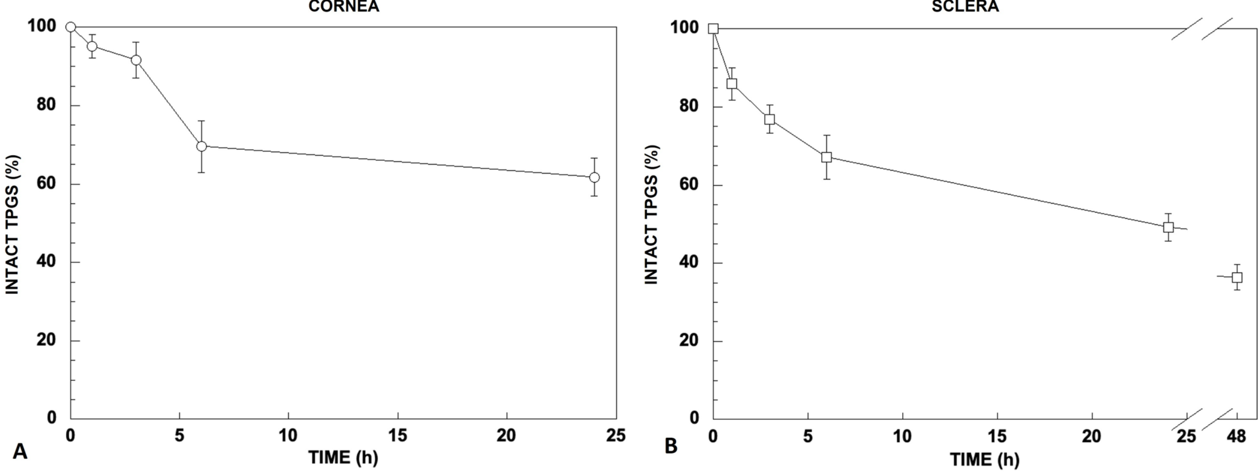

484
485
486 Figure 3. TPGS metabolism in contact with ocular tissues. Panel A: % of intact TPGS recovered after contact with the
487 cornea at 37°C; the ratio between TPGS amount (20 µg) and corneal tissue (approx. 50 mg) was around 0.4 µg/mg of
488 tissue. The data is the mean value of 12 samples from 6 different eyes. Panel B: % of intact TPGS recovered after contact
489 with the sclera at 37°C; the ratio between TPGS amount (30 µg) and scleral tissue (approx. 60 mg) was around 0.5 µg/mg
490 of tissue. The data is the mean value of 12 samples from 4 different eyes.
491
492 Overall the results obtained (Figure 3) show a decrease of TPGS concentration in contact with both
493 cornea and sclera. Although the initial partition of the polymer in the tissue, we can reasonably
494 hypothesize that this reduction was due to enzymatic degradation since no TPGS reduction occurred
495 in absence of tissues (control samples) and the HPLC traces highlighted the appearance of vitamin
496 E succinate and vitamin E. The peaks of these metabolites however, were not enough high and
497 resolved to be accurately quantified probably because, differently from the situation were TPGS
498 metabolism was evaluated in solution in the presence of isolated esterase [30], the formed vitamins
499 (lipophilic) can remain stacked in the tissue. Together with the time required to TPGS to penetrate
500 the tissue, the degradation profiles obtained depend on esterase concentration and activity in the
501 two tissues. The faster metabolism in the sclera, clearly visible in the first 3 hours, is in agreement

with literature data on 4-nitrophenyl acetate hydrolysis that highlight a 2-fold faster rate of sclera for comparison with cornea [54].

It is difficult to numerically compare these results with the data obtained in the permeation experiment, given the different conditions in term of TPGS concentration and TPGS/tissue ratio. However, the data collected support the presence of a relatively fast metabolism inside ocular tissue. This could help to explain the data obtained in the transscleral experiment and support cyclosporine release into the tissue owing to TPGS degradation.

It is also worth mentioning that the release of vitamin E and vitamin E succinate, potent antioxidant compounds, could have a positive effect on the treatment of various ocular diseases, although there are still conflicting reports on their efficacy [56, 57].

3.4 Two-photon microscopy of tissues stained with NR-loaded micelles

To further investigate micelles penetration, Nile Red (NR)-loaded TPGS micelles were prepared; their size resulted comparable with the blank micelles. Cornea and sclera were treated for 2 hours with the NR-loaded micelles and the tissues were then imaged with two-photon microscopy with an irradiation wavelength of 860 or 1080 nm. As reference, a saturated aqueous solution of NR was used. NR was selected due to the very poor water-solubility ~~(as cyclosporine)~~; additionally, its emission spectrum is sensitive to the environment polarity [58]. NR, despite being a lipophilic probe, has notable differences in structure and MW if compared to cyclosporine. This means that we cannot claim that the behavior of NR-loaded micelles will be exactly the same as the drug-loaded micelles. However, the data obtained with NR can contribute to understand the behavior of micelles, when combined with the results obtained using all other techniques.

3.4.1. Two-photon microscopy of corneal tissue stained with NR-loaded micelles

Two-photon microscopy is an advanced technique, allowing for in-depth 3D visualization of biological tissues without sample handling (*i.e.* fixation, processing, sectioning, staining). In fact, the specimen is simply fit into a sample holder, moistened with saline solution to avoid dehydration, and immediately observed. In addition, in comparison to conventional fluorescence or confocal microscopy, two-photon microscopy uses less energetic photons (in the red and near-infrared region) thus reducing the photodamage that is instead typically caused by UV and visible light. Finally, specific asymmetric structures (*e.g.* collagen fibers) can be selectively imaged exploting the process of second-harmonic generation [59]. Figure 4 collects the images of the corneal epithelium and the upper stroma after 2 hours treatment with NR-loaded micelles and with a reference NR aqueous solution, when excited at 860 nm. In these conditions, NR is mainly detected in the red channel, while the corneal epithelium gives an autofluorescence signal which falls primarily in the green spectral region. The stroma is blue, due to the second harmonic generation signal (that falls at 430 nm at this excitation wavelength) typical of collagen fibers [60], while the presence of fibroblasts is clearly marked by NR accumulation.

542

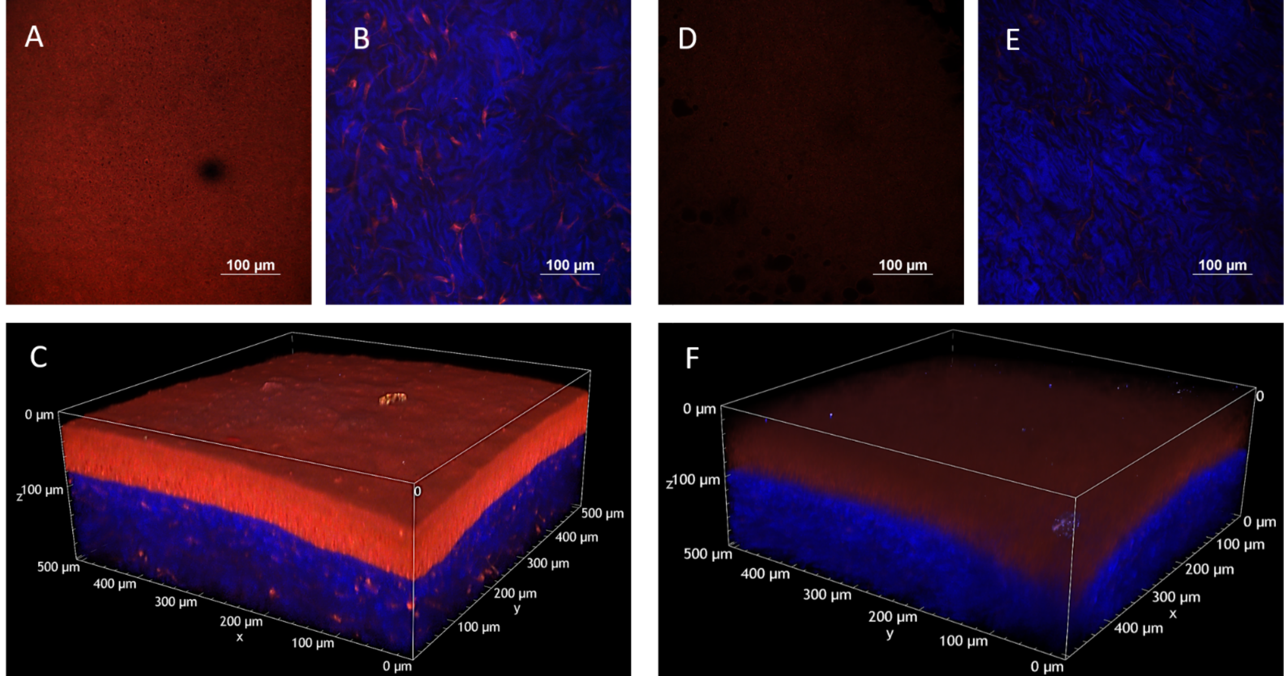

543 Figure 4. Volume renderings of corneal tissue (epithelium side) reconstructed from Z-stack, acquired with an excitation
544 wavelength of 860 nm (SHG from collagen in blue, NR fluorescence detected in both red and green channels). Panel A-
545 C: sample treated with TPGS micelles loaded with NR (Z-step: 1 µm, total depth: 202 µm). Panels A and B: XY scans
546 collected at 40 and 300 µm depth, respectively; panel C: 3D overview; Panel D-F: reference treated with NR saturated
547 aqueous solution (Z-step: 1 µm, total depth: 202 µm). Panels D and E: XY scans collected at 40 and 300 µm depth,
548 respectively, panel F: 3D overview. All the images in the two Z-scans were acquired with the same detector gains and
549 laser power.

550 The intensity of NR signal obtained with the micelles is much higher compared to the reference
551 solution, due to the higher fluorescent probe concentration. Similar results were obtained when
552 imaging the endothelial side of the tissues (Figure S3).
553 In order to obtain information on micelles-tissue interaction, we acquired emission spectra from
554 the tissue at specific focal planes. In fact, being NR a solvatochromic probe [58], the position of its
555 emission spectrum changes with the polarity of the environment. This permits to differentiate
556 between NR included in the micellar core and NR released and consequently located in cells and/or
557 in the intercellular matrix. Spectra were collected exciting the sample at 1080 nm, in order to
558 minimize the tissue autofluorescence and maximize at the same time the NR signal.
559 In Figure 5, the emission spectrum of NR in TPGS micelles (black dashed line) is compared with the
560 one collected from a corneal sample treated with micelles at a depth of 40 µm (i.e. in the epithelium,
561 corresponding to the image in Figure 4A) and 300 µm (i.e. in the corneal stroma, corresponding to
562 the image Figure 4B) from the corneal surface. The emission spectrum collected from the tissue is
563 shifted toward shorter wavelengths, and the shift increases with increasing depth. The observed
564 shift suggests that the probe is located in an environment having a different polarity with respect
565 to the micelles, indicating NR release from the nanocarrier. This conclusion is further supported by
566 the spectrum obtained from the tissue treated with a NR aqueous solution (green line), which is
567 superimposable with the spectrum obtained from the tissue treated with micelles (Figure 5 and
568 supplementary material Figure S4), confirming that NR is released from the nanocarrier.
569

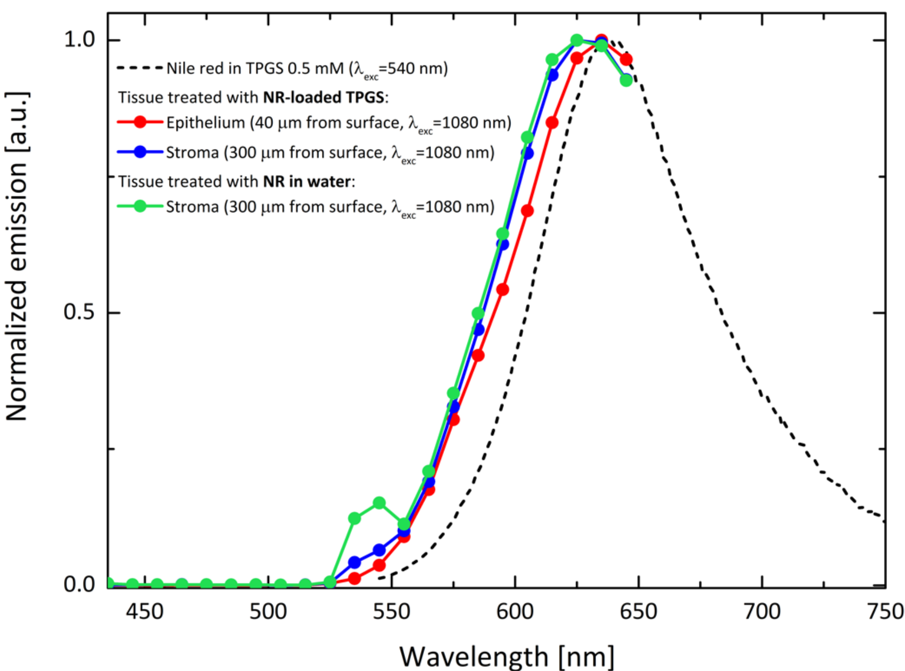

570
571 Figure 5. Comparison of the emission spectra recorded in the tissue in correspondence of the epithelium (40 µm from
572 surface, red line) and the stroma (300 µm from surface, NR-loaded TPGS: blue line, NR in water: green line) with the
573 emission profile of an aqueous solution of NR-loaded TPGS micelles recorded with a fluorometer (black dashed line).

574 The results indicate micelles disassembling in contact with the cornea, in agreement with the data
575 of TPGS and cyclosporine corneal retention discussed in par. 3.2.1.

576

577 **3.4.2. Two-photon microscopy of scleral tissue stained with NR-loaded micelles**

578

579 Figure 6 reports images obtained from a scleral sample treated for 2 hours with NR-loaded micelles,
580 upon irradiation at 860 nm. Collagen fibers appear in blue as a result of their second harmonic
581 generation (SHG) signal [61], while the red signal is given by NR fluorescence.

582

583
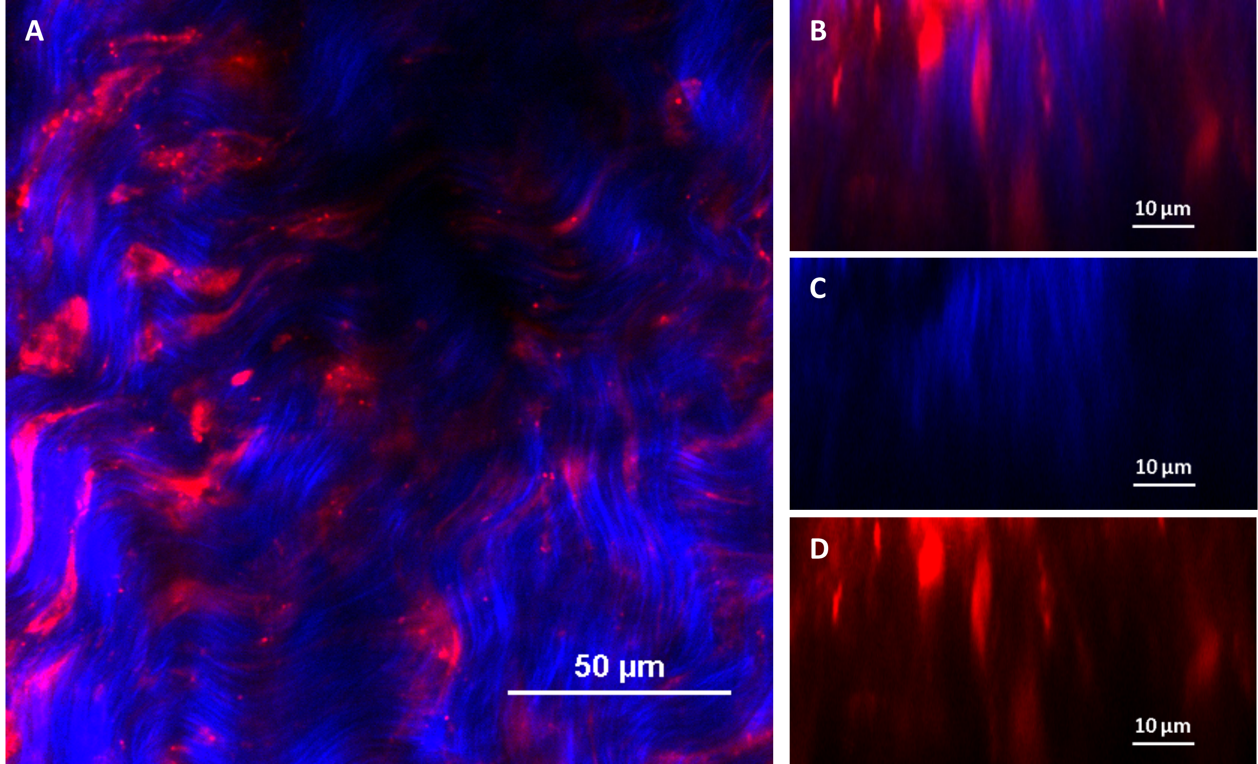

584 Figure 6. Panel A represents the scleral structure (XY plane) after treatment with NR-loaded micelles when irradiated at
585 860 nm (SHG from collagen in blue, NR fluorescence in red). Panel B (blue and red channels overlay), C (blue channel)
586 and D (red channel) represent XZ views of scleral collagen fibers extracted from a Z-stack (image size: 77 µm x 39 µm, Z
587 step: 0.42 µm).

588

589 As shown in figure 6 panel B, C and D, there is no overlap between the blue and red signals,
590 demonstrating that the fluorescent dye arranges in the interfibrillar spaces. Images were collected
591 also upon excitation at 1080 nm and again the signals of collagen fibers and NR were
592 complementary (Figure S5 in the supplementary materials).
593 As previously described for the cornea, to get further insight into micelles penetration mechanism,
594 emission spectra were recorded from the tissue. First of all, differently from the cornea, the
595 emission profile recorded from the scleral tissue after micelles application is superimposable with
596 the emission spectrum of micelles in solution (see Figure 7), indicating that the probe has not been
597 released and micelles diffuse in their intact form inside the scleral pore. Indeed, the interaction with
598 a cellular tissue such as the cornea affects micelles integrity much more than a collagen-based
599 structure such as the sclera. When the aqueous NR solution was applied to the sclera, the spectrum
600 obtained was clearly shifted toward higher wavelengths (Figure 7), indicating a more hydrophilic
601 environment, in agreement with the presence of hydrated glycosaminoglycans in the interfibrillar
602 spaces. Indeed, the profile is very similar to the one obtained with a spectrofluorometer from an
603 aqueous solution of the dye.

604

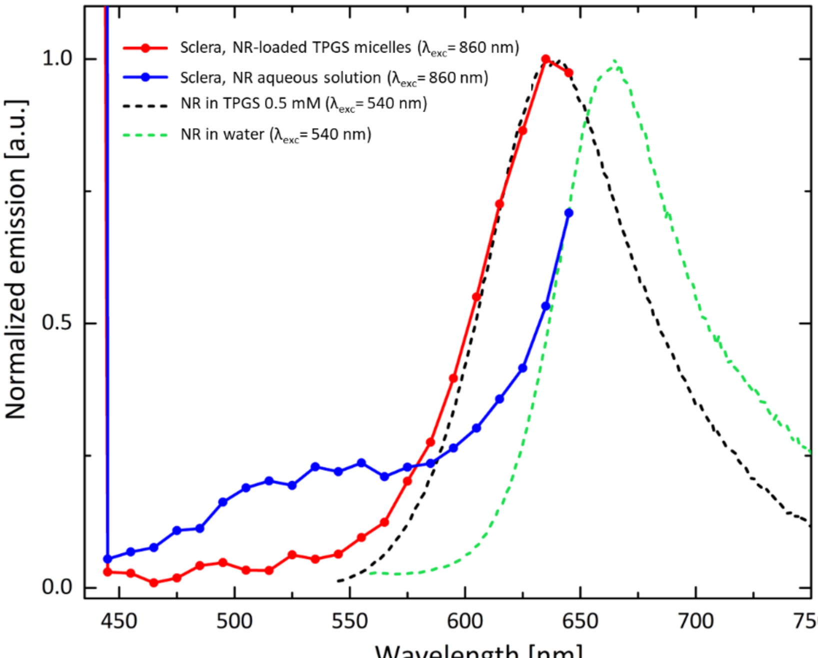

605
606 Figure 7: Emission spectrum (excitation at 860 nm) recorded in the sclera (100 µm from surface) after treatment with NR-loaded
607 TPGS micelles (red line) or the NR saturated aqueous solution (blue line); emission spectrum of NR-loaded TPGS micelles (black
608 dashed line) and NR in water (green dashed line). The last two emission spectra have been acquired using a fluorimeter.
609

610 Apparently, micelles diffuse intact across the hydrated interfibrillar matrix, and this observation is
611 in agreement with the quantification of cyclosporine and TPGS inside the sclera, which highlights
612 that the TPGS/CYC ratio found in the tissue after 6 h of contact corresponds to the one present in
613 the micellar formulation (Figure 2B).
614 Micelles diffusion occurs in the interfibrillar matrix made of negatively charged hydrated
615 proteoglycans consisting of a protein core with glycosaminoglycan (GAG) sidechains of repeating
616 disaccharide units (chondroitin, dermatan, keratan or heparin sulfate) [62, 63]. Indeed, previous
617 data have demonstrated the ability of TPGS micelles loaded with NR to diffuse intact through a
618 hyaluronic acid gel [27], possibly due to the presence of the pegylated corona [64]. The inner part
619 of the sclera is made up of thinner and more regularly arranged collagen fibers that give rise to a
620 more compact structure [65, 66]. This compact structure, together with the tortuosity of the pores
621 [67], makes it difficult for the micelles to quickly diffuse into the deepest sclera as evidenced by the
622 absence of transscleral penetration of cyclosporine after 6 hours of application; micelles can be
623 slowed down or even get stuck in the sinuous and convoluted pores. However, interaction with the
624 fibers and/or interfibrillar material together with the enzymatic hydrolysis of the TPGS, determines,
625 over a longer time, the release of cyclosporine and its delivery to the underlying tissues.
626
627

628 **3.3. Study of the effect of TPGS on cornea permeability: transcorneal permeation of**
629 **fluorescein**
630

631 Corneal retentions studies (par 3.2.1) demonstrated the permeation enhancing ability of TPGS. It is
632 however well known that penetration enhancers can also have irritative effects on the epithelium
633 and that an important requisite is linked to the possibility to quickly restore tissue barrier properties.

In this paper, we used the transcorneal flux of a probe, sodium fluorescein, to assess possible changes in the tissue permeability determined by TPGS application. Specifically, the cornea was pre-treated with TPGS 20 mM (i.e. 3% p/v) for 10 minutes, the solution was then removed, the tissue was rinsed and the permeability of sodium fluorescein was measured. As negative control, a pre-treatment of 10 minutes with HEPES buffer was used. As positive control, a concentrated (0.1% p/v) benzalkonium chloride solution was applied.
The permeability coefficients obtained are reported in Table 4. The pre-treatment with HEPES buffer gave a fluorescein permeability coefficient comparable with the previously published data (5.00 ± 4.29 x 10^{-7} cm/s) [31], while the use of a concentrated benzalkonium chloride solution demonstrated to induce a substantial increase in corneal permeability even after only 5 minutes application, in agreement with literature data [68]. TPGS 20 mM gave a permeability coefficient not statistically different from the control, confirming a reversible effect at least after 10 minutes application.

Table 4. Permeability coefficient (x 10^{-7}) cm/s of fluorescein sodium across the sclera after pre-treatment with various excipients.

PRE-TREATMENT	Permeability coefficient (x 10^{-7}) cm/s
HEPES buffer, 10 min	5.01 ± 3.32
TPGS 20 mM (3%), 10 min	9.83 ± 5.05
Benzalkonium chloride 0.1%, 5 min[a]	28.72 ± 1.65**
Benzalkonium chloride 0.1%, 10 min [a]	55.5 ± 2.07**

[a]n=2, **statistically different from the HEPES buffer (p<0.001)

This application time was selected to better mimic the *in-vivo* conditions characterized by a limited formulation-tissue contact time. Despite the promising result, the evaluation of the irritation potential is quite complex and can only be performed in vivo and after chronic application. There is however some encouraging evidence on the good tolerability of this polymer, given by the commercialization of medical devices containing this compound (Ribocross®; Coqun®) even if at lower concentration.

3. Conclusion

The combination of permeation/retention data, hydrolysis results, and two-photon microscopy images demonstrated the different interaction between ~~nano~~micelles and the two different tissues. Upon contact with the cornea, micelles disassemble and cyclosporin is probably uptaken as a free molecule. On the contrary, they can penetrate intact into the sclera, at least in the outermost part of the tissue, characterized by larger collagen fibers, organized in rather irregular bundles. The interaction of the micelles with the fibers and with the interfibrillar material together with the enzymatic hydrolysis of the TPGS, determines, in a longer time, the release of cyclosporine and its transscleral diffusion. The transscleral transport of intact micelles to the choroidal side cannot be demonstrated by our data, even if it cannot be completely excluded.
Overall, TPGS micelles are a very interesting vehicle for cyclosporin ocular delivery, since they are a water-based formulation with very low irritation potential. They efficiently promote drug permeation and retention within cornea and sclera and, in the last case, can form a drug reservoir

into the tissue that can sustain drug release into deeper tissues for an extended time. This, together with the relatively high drug concentration, could reduce administration frequency thus increasing patient's compliance. Additionally, TPGS hydrolysis determines vitamin E and vitamin E succinate release, with an antioxidant activity that can potentially contribute to the improvement of oxidation-mediated diseases. Finally, it is worth mentioning the easy preparation procedure, the possibility of sterilization by filtration and the good stability.

Authors contributions

Martina Ghezzi: conceptualization, methodology, investigation, writing-original draft preparation, writing - review and editing; Ilaria Ferraboschi: investigation, writing – review and editing; Andrea Delledonne: methodology, investigation, writing – review and editing; Silvia Pescina: methodology, validation, writing – review and editing; Cristina Padula: validation, writing – review and editing; Patrizia Santi: writing – review and editing, funding acquisition; Cristina Sissa: validation, writing – review and editing, funding acquisition; Francesca Terenziani: methodology, writing – review and editing, funding acquisition; Sara Nicoli: conceptualization, methodology, writing - original draft preparation, writing - review and editing, funding acquisition. All authors have read and agreed to the published version of the manuscript.

Funding

This work was supported by a Grant from the Italian Ministry of Research (Grant PRIN 2017 # 20173ZECCM Tackling biological barriers to antigen delivery by nanotechnological vaccines (NanoTechVax). Andrea Delledonne, Ilaria Ferraboschi, Cristina Sissa and Francesca Terenziani benefited from the equipment and support of the COMP-HUB Initiative, funded by the "Departments of Excellence" program of the Italian Ministry for Education, University and Research (MIUR, 2018–2022). We acknowledge the financial support of the University of Parma (Bando di accesso al Fondo Attrezzature Scientifiche 2018), for the purchase of the two-photon microscopy facility. Ilaria Ferraboschi benefited of a PhD fellowship financed by PON R&I 2014-2020 (FSE REACT-EU fundings). This work has received funding from the European Union's Horizon 2020 research and innovation programme under the Marie Skłodowka-Curie grant agreement No 101007804 (Micro4Nano).

Acknowledgments

Authors gratefully thank Pierugo Cavallini and Macello Annoni SpA for kindly providing porcine eye bulbs. Former undergraduate students Daisy Sorgi, Alessia Filippini and Francesca Di Pancrazio are gratefully acknowledged for their contribution in data collection.

Declaration of competing interest

The authors declare that they have no known competing financial interests or personal relationships that could have appeared to influence the work reported in this paper.

714

715 **Disclosures**

716 Partially presented (poster) at PBP World Meeting 2022, Rotterdam, 28-31 March 2022: "Micelles-
717 loaded polymeric films to improve cyclosporine solubility and ocular delivery to the posterior
718 segment", M. Ghezzi, S. Pescina, C. Padula, P. Santi, S. Nicoli.

719

720 References:

721 [1] M. Krönke, W.J. Leonard, J.M. Depper, S.K. Arya, F. Wong-Staal, R.C. Gallo, T.A. Waldmann, W.C.
722 Greene, Cyclosporin A inhibits T-cell growth factor gene expression at the level of mRNA
723 transcription, Proceedings of the National Academy of Sciences, 81 (1984) 5214.
724 [2] V. Gupta, P.K. Sahu, Topical cyclosporin A in the management of vernal keratoconjunctivitis, Eye,
725 15 (2001) 39-41.
726 [3] S. Tatlipinar, E.K. Akpek, Topical ciclosporin in the treatment of ocular surface disorders, The
727 British journal of ophthalmology, 89 (2005) 1363-1367.
728 [4] S.N. Rao, Comparison of the Efficacy of Topical Cyclosporine 0.05% Compared With Tobradex for
729 the Treatment of Posterior Blepharitis, Investigative Ophthalmology & Visual Science, 46 (2005)
730 2662-2662.
731 [5] M. Rubin, S.N. Rao, Efficacy of Topical Cyclosporin 0.05% in the Treatment of Posterior
732 Blepharitis, Journal of Ocular Pharmacology and Therapeutics, 22 (2006) 47-53.
733 [6] A.T. Vitale, A. Rodriguez, C.S. Foster, Low-dose Cyclosporin A Therapy in Treating Chronic,
734 Noninfectious Uveitis, Ophthalmology, 103 (1996) 365-374.
735 [7] R.J. Barry, Q.D. Nguyen, R.W. Lee, P.I. Murray, A.K. Denniston, Pharmacotherapy for uveitis:
736 current management and emerging therapy, Clinical ophthalmology (Auckland, N.Z.), 8 (2014) 1891-
737 1911.
738 [8] Z. Saleh, T. Arayssi, Update on the therapy of Behçet disease, Therapeutic Advances in Chronic
739 Disease, 5 (2014) 112-134.
740 [9] F. Lallemand, O. Felt-Baeyens, K. Besseghir, F. Behar-Cohen, R. Gurny, Cyclosporine A delivery to
741 the eye: A pharmaceutical challenge, European Journal of Pharmaceutics and Biopharmaceutics, 56
742 (2003) 307-318.
743 [10] N. El Tayar, A.E. Mark, P. Vallat, R.M. Brunne, B. Testa, W.F. van Gunsteren, Solvent-dependent
744 conformation and hydrogen-bonding capacity of cyclosporin A: evidence from partition coefficients
745 and molecular dynamics simulations, Journal of Medicinal Chemistry, 36 (1993) 3757-3764.
746 [11] F. Lallemand, M. Schmitt, J.-L. Bourges, R. Gurny, S. Benita, J.-S. Garrigue, Cyclosporine A
747 delivery to the eye: A comprehensive review of academic and industrial efforts, European Journal
748 of Pharmaceutics and Biopharmaceutics, 117 (2017) 14-28.
749 [12] A. Patel, K. Cholkar, V. Agrahari, A.K. Mitra, Ocular drug delivery systems: An overview, World
750 journal of pharmacology, 2 (2013) 47-64.
751 [13] M. Ghezzi, S. Pescina, C. Padula, P. Santi, E. Del Favero, L. Cantù, S. Nicoli, Polymeric micelles in
752 drug delivery: An insight of the techniques for their characterization and assessment in biorelevant
753 conditions, Journal of Controlled Release, 332 (2021) 312-336.
754 [14] Polymeric micelles for ocular drug delivery: From structural frameworks to recent preclinical
755 studies, Journal of Controlled Release, 248 (2017) 96 - 116.
756 [15] M.A. Toscanini, M.J. Limeres, A.V. Garrido, M. Cagel, E. Bernabeu, M.A. Moretton, D.A.
757 Chiappetta, M.L. Cuestas, Polymeric micelles and nanomedicines: Shaping the future of next
758 generation therapeutic strategies for infectious diseases, Journal of Drug Delivery Science and
759 Technology, 66 (2021) 102927.

760 [16] M.A. Grimaudo, S. Pescina, C. Padula, P. Santi, A. Concheiro, C. Alvarez-Lorenzo, S. Nicoli,
761 Topical application of polymeric nanomicelles in ophthalmology: a review on research efforts for
762 the noninvasive delivery of ocular therapeutics, Expert Opinion on Drug Delivery, 16 (2019) 397-
763 413.
764 [17] Y. Yu, D. Chen, Y. Li, W. Yang, J. Tu, Y. Shen, Improving the topical ocular pharmacokinetics of
765 lyophilized cyclosporine A-loaded micelles: formulation, in vitro and in vivo studies, Drug delivery,
766 25 (2018) 888-899.
767 [18] A. Varela-Garcia, A. Concheiro, C. Alvarez-Lorenzo, Soluplus micelles for acyclovir ocular
768 delivery: Formulation and cornea and sclera permeability, International Journal of Pharmaceutics,
769 552 (2018) 39-47.
770 [19] Z. Li, M. Liu, L. Ke, L.-J. Wang, C. Wu, C. Li, Z. Li, Y.-L. Wu, Flexible polymeric nanosized micelles
771 for ophthalmic drug delivery: research progress in the last three years, Nanoscale Advances, 3
772 (2021) 5240-5254.
773 [20] C. Di Tommaso, J.-L. Bourges, F. Valamanesh, G. Trubitsyn, A. Torriglia, J.-C. Jeanny, F. Behar-
774 Cohen, R. Gurny, M. Möller, Novel micelle carriers for cyclosporin A topical ocular delivery: In vivo
775 cornea penetration, ocular distribution and efficacy studies, European Journal of Pharmaceutics and
776 Biopharmaceutics, 81 (2012) 257-264.
777 [21] R.D. Vaishya, M. Gokulgandhi, S. Patel, M. Minocha, A.K. Mitra, Novel Dexamethasone-Loaded
778 Nanomicelles for the Intermediate and Posterior Segment Uveitis, AAPS PharmSciTech, 15 (2014)
779 1238-1251.
780 [22] N. Elsaid, S. Somavarapu, T.L. Jackson, Cholesterol-poly(ethylene) glycol nanocarriers for the
781 transscleral delivery of sirolimus, Experimental Eye Research, 121 (2014) 121-129.
782 [23] C. Peng, L. Kuang, J. Zhao, A.E. Ross, Z. Wang, J.B. Ciolino, Bibliometric and visualized analysis
783 of ocular drug delivery from 2001 to 2020, Journal of Controlled Release, 345 (2022) 625-645.
784 [24] Polymeric micelles in mucosal drug delivery: Challenges towards clinical translation,
785 Biotechnology Advances, 33 (2015) 1380 - 1392.
786 [25] Y. Wang, L. Jiang, Q. Shen, J. Shen, Y. Han, H. Zhang, Investigation on the self-assembled
787 behaviors of C18 unsaturated fatty acids in arginine aqueous solution, RSC Advances, 7 (2017)
788 41561-41572.
789 [26] A.-L. Fameau, A. Arnould, A. Saint-Jalmes, Responsive self-assemblies based on fatty acids,
790 Current Opinion in Colloid & Interface Science, 19 (2014) 471-479.
791 [27] M. Ghezzi, S. Pescina, A. Delledonne, I. Ferraboschi, C. Sissa, F. Terenziani, P.D.F.R. Remiro, P.
792 Santi, S. Nicoli, Improvement of Imiquimod Solubilization and Skin Retention via TPGS Micelles:
793 Exploiting the Co-Solubilizing Effect of Oleic Acid, Pharmaceutics, 13 (2021) 1476.
794 [28] S. Tampucci, L. Guazzelli, S. Burgalassi, S. Carpi, P. Chetoni, A. Mezzetta, P. Nieri, B. Polini, C.S.
795 Pomelli, E. Terreni, D. Monti, pH-Responsive Nanostructures Based on Surface Active Fatty Acid-
796 Protic Ionic Liquids for Imiquimod Delivery in Skin Cancer Topical Therapy, Pharmaceutics, 12 (2020)
797 1078.
798 [29] G. Ismailos, C. Reppas, J.B. Dressman, P. Macheras, Unusual solubility behaviour of cyclosporin
799 A in aqueous media, Journal of Pharmacy and Pharmacology, 43 (1991) 287-289.
800 [30] M.A. Grimaudo, S. Pescina, C. Padula, P. Santi, A. Concheiro, C. Alvarez-Lorenzo, S. Nicoli,
801 Poloxamer 407/TPGS Mixed Micelles as Promising Carriers for Cyclosporine Ocular Delivery, Mol
802 Pharm, 15 (2018) 571-584.
803 [31] S. Pescina, P. Govoni, A. Potenza, C. Padula, P. Santi, S. Nicoli, Development of a Convenient ex
804 vivo Model for the Study of the Transcorneal Permeation of Drugs: Histological and Permeability
805 Evaluation, Journal of Pharmaceutical Sciences, 104 (2015) 63-71.

806 [32] R.D. Bachu, P. Chowdhury, Z.H.F. Al-Saedi, P.K. Karla, S.H.S. Boddu, Ocular Drug Delivery
807 Barriers—Role of Nanocarriers in the Treatment of Anterior Segment Ocular Diseases,
808 Pharmaceutics, 10 (2018) 28.
809 [33] C. Ostacolo, C. Caruso, D. Tronino, S. Troisi, S. Laneri, L. Pacente, A. Del Prete, A. Sacchi,
810 Enhancement of corneal permeation of riboflavin-5′-phosphate through vitamin E TPGS: A
811 promising approach in corneal trans-epithelial cross linking treatment, International Journal of
812 Pharmaceutics, 440 (2013) 148-153.
813 [34] M.H. Warsi, M. Anwar, V. Garg, G.K. Jain, S. Talegaonkar, F.J. Ahmad, R.K. Khar, Dorzolamide-
814 loaded PLGA/vitamin E TPGS nanoparticles for glaucoma therapy: Pharmacoscintigraphy study and
815 evaluation of extended ocular hypotensive effect in rabbits, Colloids and Surfaces B: Biointerfaces,
816 122 (2014) 423-431.
817 [35] M. Alkholief, H. Albasit, A. Alhowyan, S. Alshehri, M. Raish, M. Abul Kalam, A. Alshamsan,
818 Employing a PLGA-TPGS based nanoparticle to improve the ocular delivery of Acyclovir, Saudi
819 Pharmaceutical Journal, 27 (2019) 293-302.
820 [36] E.-M. Collnot, C. Baldes, M.F. Wempe, R. Kappl, J. Hüttermann, J.A. Hyatt, K.J. Edgar, U.F.
821 Schaefer, C.-M. Lehr, Mechanism of Inhibition of P-Glycoprotein Mediated Efflux by Vitamin E TPGS:
822 Influence on ATPase Activity and Membrane Fluidity, Molecular Pharmaceutics, 4 (2007) 465-474.
823 [37] A.W.G. Alani, D.A. Rao, R. Seidel, J. Wang, J. Jiao, G.S. Kwon, The Effect of Novel Surfactants and
824 Solutol® HS 15 on Paclitaxel Aqueous Solubility and Permeability Across a Caco-2 Monolayer, Journal
825 of Pharmaceutical Sciences, 99 (2010) 3473-3485.
826 [38] L. Song, Y. Shen, J. Hou, L. Lei, S. Guo, C. Qian, Polymeric micelles for parenteral delivery of
827 curcumin: Preparation, characterization and in vitro evaluation, Colloids and Surfaces A:
828 Physicochemical and Engineering Aspects, 390 (2011) 25-32.
829 [39] N.F. Younes, S.A. Abdel-Halim, A.I. Elassasy, Solutol HS15 based binary mixed micelles with
830 penetration enhancers for augmented corneal delivery of sertaconazole nitrate: optimization, in
831 vitro, ex vivo and in vivo characterization, Drug Delivery, 25 (2018) 1706-1717.
832 [40] P.F. Hoyng, N. Verbey, L. Thörig, N.J. van Haeringen, Topical prostaglandins inhibit trauma-
833 induced inflammation in the rabbit eye, Investigative Ophthalmology & Visual Science, 27 (1986)
834 1217-1225.
835 [41] A. Macrì, S. Giuffrida, V. Amico, M. Iester, C.E. Traverso, Effect of linoleic acid and γ-linolenic
836 acid on tear production, tear clearance and on the ocular surface after photorefractive keratectomy,
837 Graefe's Archive for Clinical and Experimental Ophthalmology, 241 (2003) 561-566.
838 [42] S. Barabino, M. Rolando, P. Camicione, G. Ravera, S. Zanardi, S. Giuffrida, G. Calabria, Systemic
839 Linoleic and γ-Linolenic Acid Therapy in Dry Eye Syndrome With an Inflammatory Component,
840 Cornea, 22 (2003).
841 [43] I. Molina-Leyva, A. Molina-Leyva, A. Bueno-Cavanillas, Efficacy of nutritional supplementation
842 with omega-3 and omega-6 fatty acids in dry eye syndrome: a systematic review of randomized
843 clinical trials, Acta Ophthalmologica, 95 (2017) e677-e685.
844 [44] J.S. Fogt, N. Fogt, P.E. King-Smith, H. Liu, J.T. Barr, Changes in Tear Lipid Layer Thickness and
845 Symptoms Following the Use of Artificial Tears with and Without Omega-3 Fatty Acids: A
846 Randomized, Double-Masked, Crossover Study, Clinical ophthalmology (Auckland, N.Z.), 13 (2019)
847 2553-2561.
848 [45] S. Rashid, Y. Jin, T. Ecoiffier, S. Barabino, D.A. Schaumberg, M.R. Dana, Topical Omega-3 and
849 Omega-6 Fatty Acids for Treatment of Dry Eye, Archives of Ophthalmology, 126 (2008) 219-225.
850 [46] S. Pescina, L.G. Lucca, P. Govoni, C. Padula, E.D. Favero, L. Cantù, P. Santi, S. Nicoli, Ex Vivo
851 Conjunctival Retention and Transconjunctival Transport of Poorly Soluble Drugs Using Polymeric
852 Micelles, Pharmaceutics, 11 (2019) 476.

[47] S. Shubber, D. Vllasaliu, C. Rauch, F. Jordan, L. Illum, S. Stolnik, Mechanism of mucosal permeability enhancement of CriticalSorb® (Solutol® HS15) investigated in vitro in cell cultures, Pharmaceutical research, 32 (2015) 516-527.
[48] I. Pepić, J. Lovrić, J. Filipović-Grčić, How do polymeric micelles cross epithelial barriers?, European Journal of Pharmaceutical Sciences, 50 (2013) 42-55.
[49] M.S. Shahab, M. Rizwanullah, S. Sarim Imam, Formulation, optimization and evaluation of vitamin E TPGS emulsified dorzolamide solid lipid nanoparticles, Journal of Drug Delivery Science and Technology, 68 (2022) 103062.
[50] A. Labbé, C. Baudouin, D. Ismail, M. Amrane, J.S. Garrigue, A. Leonardi, F.C. Figueiredo, G. Van Setten, M. Labetoulle, Pan-European survey of the topical ocular use of cyclosporine A, Journal Français d'Ophtalmologie, 40 (2017) 187-195.
[51] E. Eljarrat-Binstock, J. Pe'er, A.J. Domb, New Techniques for Drug Delivery to the Posterior Eye Segment, Pharmaceutical Research, 27 (2010) 530-543.
[52] M.G. Traber, C.A. Thellman, M.J. Rindler, H.J. Kayden, Uptake of intact TPGS (d-alpha-tocopheryl polyethylene glycol 1000 succinate) a water-miscible form of vitamin E by human cells in vitro, The American Journal of Clinical Nutrition, 48 (1988) 605-611.
[53] S. Duvvuri, S. Majumdar, K.A. Mitra, Role of Metabolism in Ocular Drug Delivery, Current Drug Metabolism, 5 (2004) 507-515.
[54] E.M. Heikkinen, E.M. del Amo, V.-P. Ranta, A. Urtti, K.-S. Vellonen, M. Ruponen, Esterase activity in porcine and albino rabbit ocular tissues, European Journal of Pharmaceutical Sciences, 123 (2018) 106-110.
[55] P. Ichhpujani, L.J. Katz, G. Hollo, C.L. Shields, J.A. Shields, B. Marr, R. Eagle, H. Alvim, S.S. Wizov, A. Acheampong, J. Chen, L.A. Wheeler, Comparison of Human Ocular Distribution of Bimatoprost and Latanoprost, Journal of Ocular Pharmacology and Therapeutics, 28 (2011) 134-145.
[56] A.K. Grover, S.E. Samson, Antioxidants and vision health: facts and fiction, Molecular and Cellular Biochemistry, 388 (2014) 173-183.
[57] M.M. McCusker, K. Durrani, M.J. Payette, J. Suchecki, An eye on nutrition: The role of vitamins, essential fatty acids, and antioxidants in age-related macular degeneration, dry eye syndrome, and cataract, Clinics in Dermatology, 34 (2016) 276-285.
[58] B. Boldrini, E. Cavalli, A. Painelli, F. Terenziani, Polar Dyes in Solution: A Joint Experimental and Theoretical Study of Absorption and Emission Band Shapes, The Journal of Physical Chemistry A, 106 (2002) 6286-6294.
[59] F. Helmchen, W. Denk, Deep tissue two-photon microscopy, Nature Methods, 2 (2005) 932-940.
[60] C.Y. Park, J.K. Lee, R.S. Chuck, Second Harmonic Generation Imaging Analysis of Collagen Arrangement in Human Cornea, Investigative Ophthalmology & Visual Science, 56 (2015) 5622-5629.
[61] M. Zyablitskaya, E.L. Munteanu, T. Nagasaki, D.C. Paik, Second Harmonic Generation Signals in Rabbit Sclera As a Tool for Evaluation of Therapeutic Tissue Cross-linking (TXL) for Myopia, Journal of visualized experiments : JoVE, (2018) 56385.
[62] P.G. Watson, R.D. Young, Scleral structure, organisation and disease. A review, Experimental Eye Research, 78 (2004) 609-623.
[63] J.G. Hollyfield, M.E. Rayborn, M. Tammi, R. Tammi, Hyaluronan in the Interphotoreceptor Matrix of the Eye: Species Differences in Content, Distribution, Ligand Binding and degradation, Experimental Eye Research, 66 (1998) 241-248.
[64] J. Puig-Rigall, C. Fernández-Rubio, J. González-Benito, J.E. Houston, A. Radulescu, P. Nguewa, G. González-Gaitano, Structural characterization by scattering and spectroscopic methods and

900 biological evaluation of polymeric micelles of poloxamines and TPGS as nanocarriers for miltefosine
901 delivery, International Journal of Pharmaceutics, 578 (2020) 119057.
902 [65] J.K. Pijanka, B. Coudrillier, K. Ziegler, T. Sorensen, K.M. Meek, T.D. Nguyen, H.A. Quigley, C.
903 Boote, Quantitative Mapping of Collagen Fiber Orientation in Non-glaucoma and Glaucoma
904 Posterior Human Sclerae, Investigative Ophthalmology & Visual Science, 53 (2012) 5258-5270.
905 [66] Y. Komai, T. Ushiki, The three-dimensional organization of collagen fibrils in the human cornea
906 and sclera, Investigative Ophthalmology & Visual Science, 32 (1991) 2244-2258.
907 [67] K.M. Hämäläinen, K. Kananen, S. Auriola, K. Kontturi, A. Urtti, Characterization of paracellular
908 and aqueous penetration routes in cornea, conjunctiva, and sclera, Investigative Ophthalmology &
909 Visual Science, 38 (1997) 627-634.
910 [68] W. Chen, Z. Li, J. Hu, Z. Zhang, L. Chen, Y. Chen, Z. Liu, Corneal Alternations Induced by Topical
911 Application of Benzalkonium Chloride in Rabbit, PLOS ONE, 6 (2011) e26103.
912 [69] E. Donnenfeld, S.C. Pflugfelder, Topical Ophthalmic Cyclosporine: Pharmacology and Clinical
913 Uses, Survey of Ophthalmology, 54 (2009) 321-338.
914 [70] G.J. Jaffe, C.-S. Yang, X.-C. Wang, S.W. Cousins, R.P. Gallemore, P. Ashton, Intravitreal sustained-
915 release cyclosporine in the treatment of experimental uveitis, Ophthalmology, 105 (1998) 46-56.
916